Supporting information

Novel Diacid-superbase Ionic Liquids for Efficient Dissolving Cellulose and Simultaneous Preparation of Multifunctional Cellulose Materials

Long Zhang[1], Boxiang Zhan[2], Yapeng He[3], Yongqi Deng[4], Haiyuan Ji[5], Shen Peng[6], Lifeng Yan[7*]

[1,2,3,4,5,6,7]Key Laboratory of Precision and Intelligent Chemistry, and Department of Chemical Physics, University of Science and Technology of China, Jinzhai Road 96, 230026, Hefei, Anhui, China.

Number of pages-17, tables-4, scheme-1, figures-17

Supplementary Methods

1. Determination of KT parameters[1]

Kamlet-Taft parameters (α, β, and π*) were determined using Nile Red and 4-nitroaniline as probe molecules. Specifically, the methanol solution of Nile Red and 4-nitroaniline at a concentration of 1×10^{-3} mol/L was prepared. Then, the appropriate amount of the solution was placed in a centrifuge tube and heated to remove the methanol. Subsequently, SIL was added to the centrifuge tube and mixed fully with the dye. Finally, the solution was poured into a cuvette and the absorption spectrum of the solution in the range of 350-700 nm was measured using a UV-Vis spectrophotometer.

Using Nile Red as the molecular probe, the values of π* and α were determined by the following equation.

$$\alpha = \frac{19.9657 - 1.0241 \times \pi* - V_{NR}}{1.6078}$$

$$\pi* = \frac{19.839 - V_{NR}}{2.9912}$$

Using 4-nitroaniline as the molecular probe, the value of β was determined by the following equation.

$$\beta = 11.134 - \frac{3580}{\lambda(NH2)max} - 1.125 \times \pi*$$

2. Determination of degree of polymerization (DP) of cellulose[2]

The DP of the cellulose was measured by using a viscometer in CUEN (copper (II) ethylenediamine). Firstly, the 0.5 mol L^{-1} CUEN solution was prepared and the cellulose sample was added to the solution, ensuring that the concentration of the cellulose/CUEN solution was 0.2 g/100 ml. After the dissolution of the cellulose, the efflux time was determined by the viscometer. The DP was calculated as follows:

$$\eta_r = \frac{t}{t_0}$$

η_r, relative viscosity; t, cellulose solution efflux time (s); t_0, 0.5 mol L^{-1} CUEN solution efflux time (s).

$$[\eta]' = \frac{[\eta] \times C}{C'}$$

$[\eta]'$, intrinsic viscosity; C', actual concentration of CUEN solution, $[\eta] \times C$, determined corresponding to the value of η_r.

$$DP = 190 \times [\eta]'$$

3. Porosity determination[3]

The prepared cellulose gel was freeze-dried to obtain aerogel. The average porosity of the aerogel was determined using the ethanol displacement method. Firstly, pre-weighed aerogel was immersed in anhydrous ethanol at room temperature and placed in a vacuum oven under reduced pressure (0.1 mPa) for 5 min to ensure that the ethanol completely penetrated the pores in the aerogel. The weight of the saturated aerogel was recorded immediately after it was removed from the oven. Finally, the porosity of the aerogel was calculated according to the following equation.

$$Porosity\ (\%) = \frac{W_e - W_0}{\rho_e \times V_s} \times 100\%$$

W_0 (g) and W_e (g) are the weights of the aerogel before and after immersion in ethanol, respectively. ρ_e is the density of ethanol (0.789 g/cm^3) and V_s is the volume of the aerogel (cm^3).

4. Electrochemical formula[4]

Ionic conductivity test of cellulose electrolyte was carried out in the frequency range of 0.1 HZ to 100 KHz and voltage of 5 mV. Two stainless steel meshes were placed in parallel with cellulose hydrogel sandwiched between them. The formula for calculating ionic conductivity was as follows:

$$\sigma = \frac{L}{S \times R_b}$$

where L is the distance between the two electrodes, S is the contact area between

the electrolyte and the electrodes, and Rb is the resistance determined by the first intersection with the real axis.

The capacitance (C), energy density (E), and power density (P) based on the GCD curves were calculated using the equations.

$$C = \frac{I \times t_D}{V \times M}$$

$$E = \frac{1}{2} \times C \times V^2$$

$$P = \frac{E \times 3600}{t_D}$$

where I is the discharge current, V is the potential window during the discharge after the IR drop, and t_D is the discharge time.

Table

Table S1. Solubility of cellulose by different SILs

Cationic	Anionic	Molar ratio (Cationic: Anionic)	Abbreviation (SIL)	Status (RT)	Temp (℃)	Type of cellulose	Cellulose solubility (wt%)
DBN	Ethanedioic acid	2:1	DBN-Ea	Solid	100	MCC	4.0
DBN	Malonic acid	2:1	DBN-Ma	Liquid	100	MCC	13.1
DBN	Succinic acid	2:1	DBN-Sa	Solid	100	MCC	1.5
DBN	Oxalic acid dihydrate	2:1	DBN-Oad	Solid	100	MCC	0.7
DBU	Ethanedioic acid	2:1	DBU-Ea	Solid	100	MCC	4.2
DBU	Malonic acid	2:1	DBU-Ma	Liquid	100	MCC	15.2
DBU	Succinic acid	2:1	DBU-Sa	Solid	100	MCC	2.6
DBU	Oxalic acid dihydrate	2:1	DBU-Oad	Solid	100	MCC	1.4
DBU	Malonic acid	2:1	DBU-Ma	Liquid	100	Cotton wool	9.3

Table S2. The Kamlet-Taft parameters of DBU-Ma and DBN-Ma.

Abbreviation (SIL)	α	β	$\beta - \alpha$	π^*
DBU-Ma	0.9412	1.3910	0.4498	0.7049
DBN-Ma	0.9154	1.3243	0.4089	0.6838

Table S3. Dissolving time is required for different MCC concentrations.

MCC concentration	2 wt%	4 wt%	6 wt%	8 wt%
Dissolving time	0.75 h	1.5 h	3.0 h	4.5 h

Table S4. Comparison of the present work with mono-acidic IL systems.

Solvents	Types of cellulose	Degree of polymerization	Temperature (°C)	Solubility (wt%)	References
NaOH/H$_2$O	MCC	170	-6	7.6	5
NaOH/Urea/H$_2$O	Cotton linters	410	0	5	6
ChCl/ZnCl$_2$	MCC	-	110	< 0.2	7
Acetamide/urea	Cotton-ramie pulp	517	50	1.03	8
ChCl/oxalic acid	Cotton linters	575	110	1	9
ChCl/imidazole	Cotton linters	575	110	2.5	10
ChCl/urea	Cotton linters	575	110	1.5	10
ChCl/lactic acid	Fibrous cellulose	-	60	3	11
[C$_4$mim]Cl	Dissolving pulp	1000	100	10	12
[C$_6$mim]Cl	Dissolving pulp	1000	100	5	12
[Amim][Cl]	Dissolving pulp	-	80	14.5	13
[Emim][Ac]	Dissolving pulp	500	90	16.3	14
[Bmim][Cl]	Dissolving pulp	500	90	9.5	14
[A2im][CH3COO]	MCC	275	30	17.0	15
[A2im][CH3COO]	MCC	275	50	19.5	15
[A2im][CH3CH2OCH2COO]	MCC	275	30	3.5	15
[A2im][CH3CH2OCH2COO]	MCC	275	50	19.3	15
[A2im][HOCH2COO]	MCC	275	30	0.3	15
[A2im][HOCH2COO]	MCC	275	50	1.2	15
[N(C4C1)Py][CH3OCH2COO]	MCC	275	40	1.2	15
[N(C4C1)Py][CH3OCH2COO]	MCC	275	50	15.2	15

[DBUH][CH$_3$COCH$_2$CH2COO]	MCC	280	100	16	[1]
[DBUH][CH$_3$COCH$_2$CH2COO]	bamboo cellulose	860	100	7	[1]
[DBUH][H$_2$NCH$_2$COO]	MCC	156	90	1.02	[16]
[DBUH][CH$_3$CHOHCOO]	MCC	156	90	4.94	[16]
[DBUH][CH$_2$=CCH$_3$COO]	MCC	156	90	5.92	[16]
[DBUH][HSCH$_2$COO]	MCC	156	90	7.96	[16]
[DBUH][CH$_3$CH$_2$COO]	MCC	156	90	12.64	[16]
[DBUH][CH$_3$COO]	MCC	156	90	14.80	[16]
[DBUH][CH$_2$=CHCOO]	MCC	156	90	15.37	[16]
[DBUH][HCOO]	MCC	156	90	18.92	[16]
[DBNH][CH$_3$CH$_2$COO]	MCC	156	90	12.34	[16]
[DBNH][CH$_3$COO]	MCC	156	90	14.70	[16]
[DBNH][CH$_2$=CHCOO]	MCC	156	90	14.88	[16]
[DBNH][HCOO]	MCC	156	90	17.06	[16]
DBU-Ma	MCC	260	100	15.2	This work
DBN-Ma	MCC	260	100	13.1	This work
DBU-Ma	Cotton wool	685	100	9.3	This work

Scheme
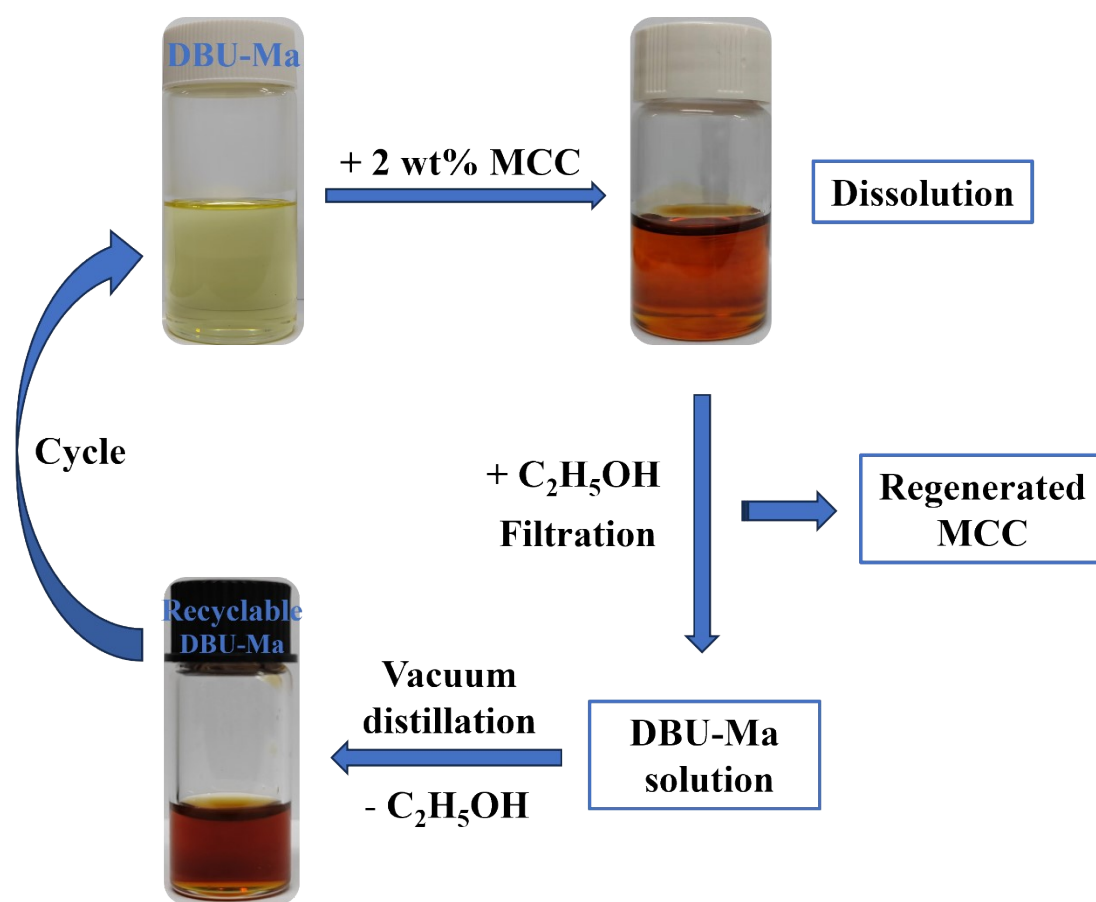
Scheme S1. The scheme for SILs recycling.

Figure

DBN-Ea **DBN-Ma** **DBN-Sa** **DBN-Oad**

DBU-Ea **DBU-Ma** **DBU-Sa** **DBU-Oad**
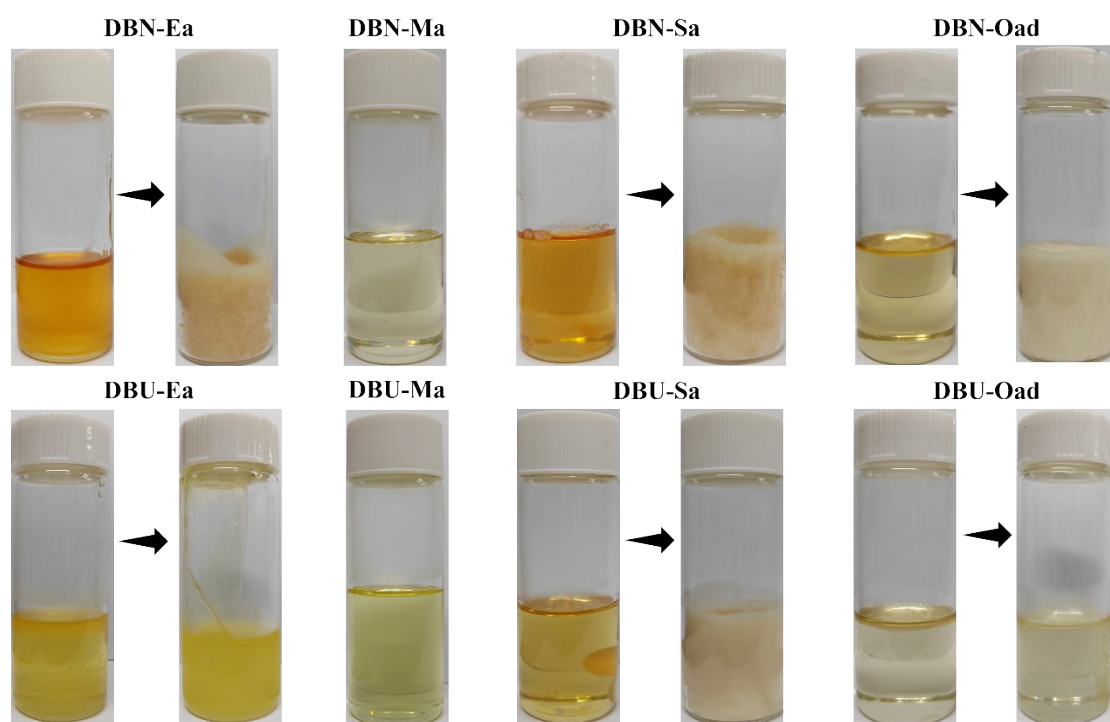
Figure S1. Photographs of eight SILs.
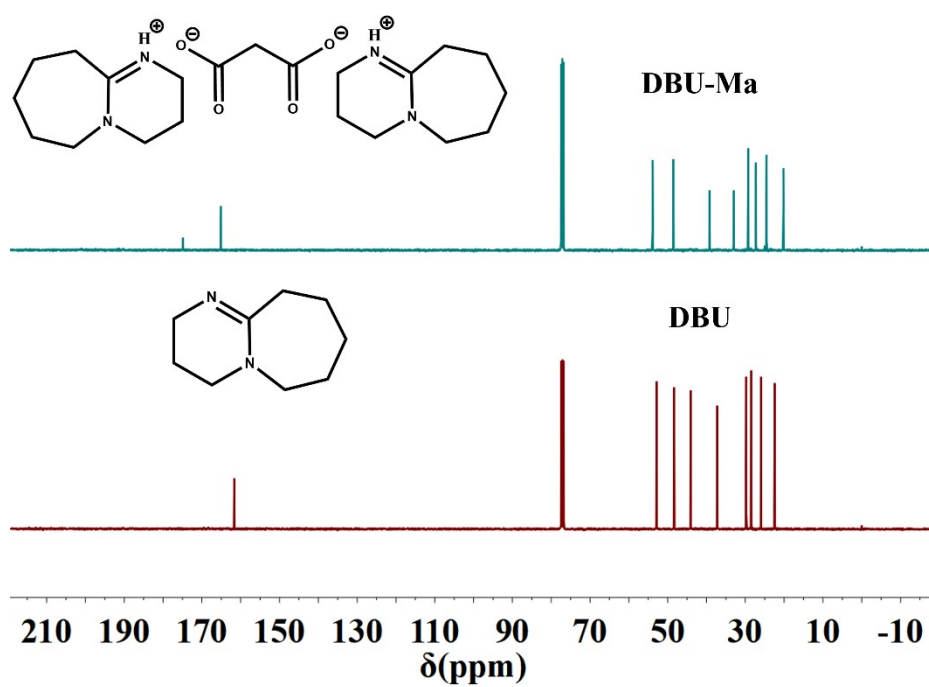
Figure S2. ^{13}C NMR of DBN-Ma and DBU.
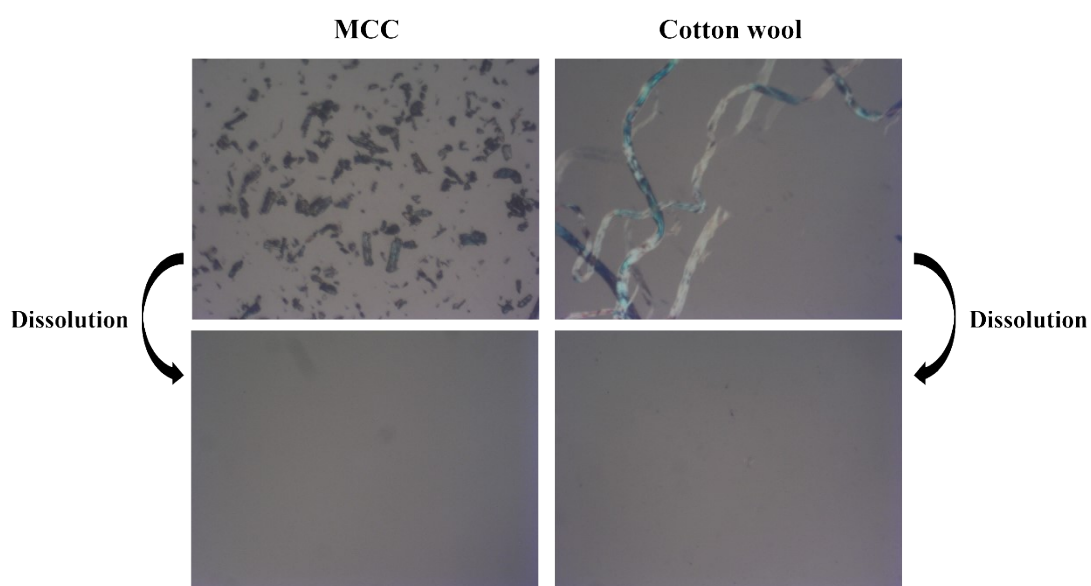
Figure S3. Microscopic photographs of MCC and cotton wool.

.
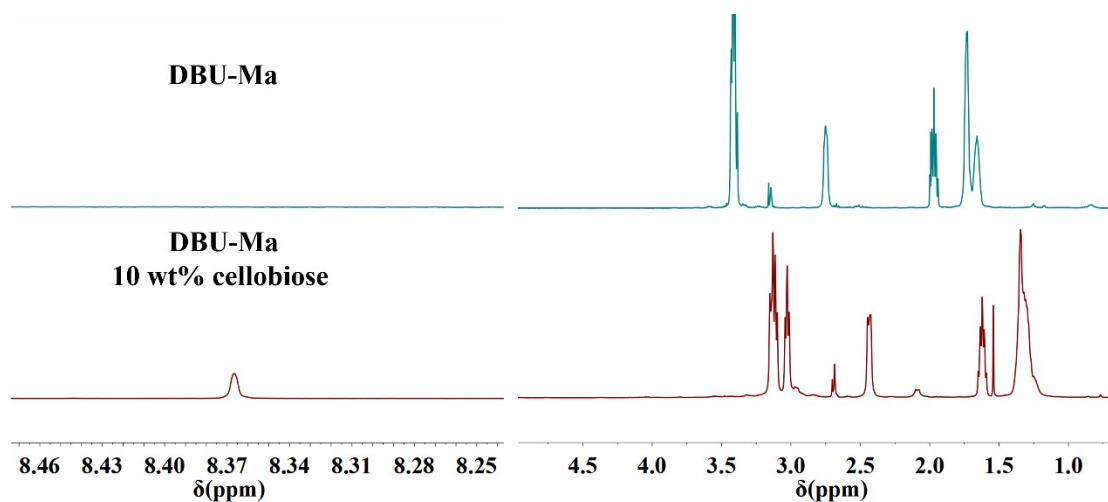
Figure S4. ^{1}H NMR of DBU-Ma of 10 wt% cellobiose and DBU-Ma.
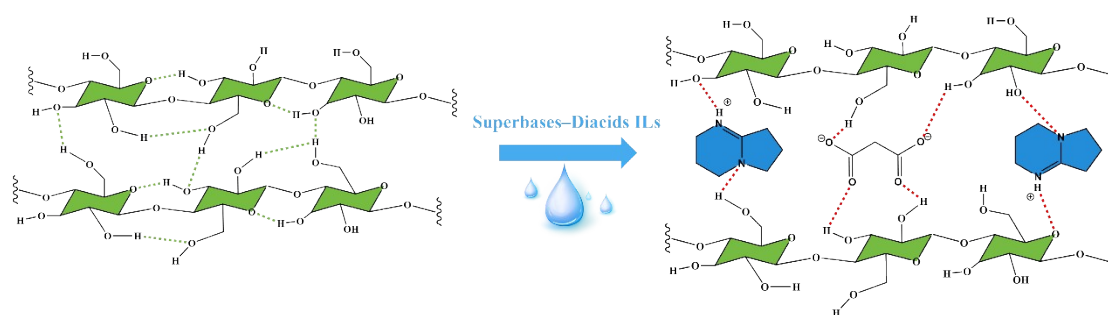
Figure S5. The mechanism of cellulose dissolution by SILs.
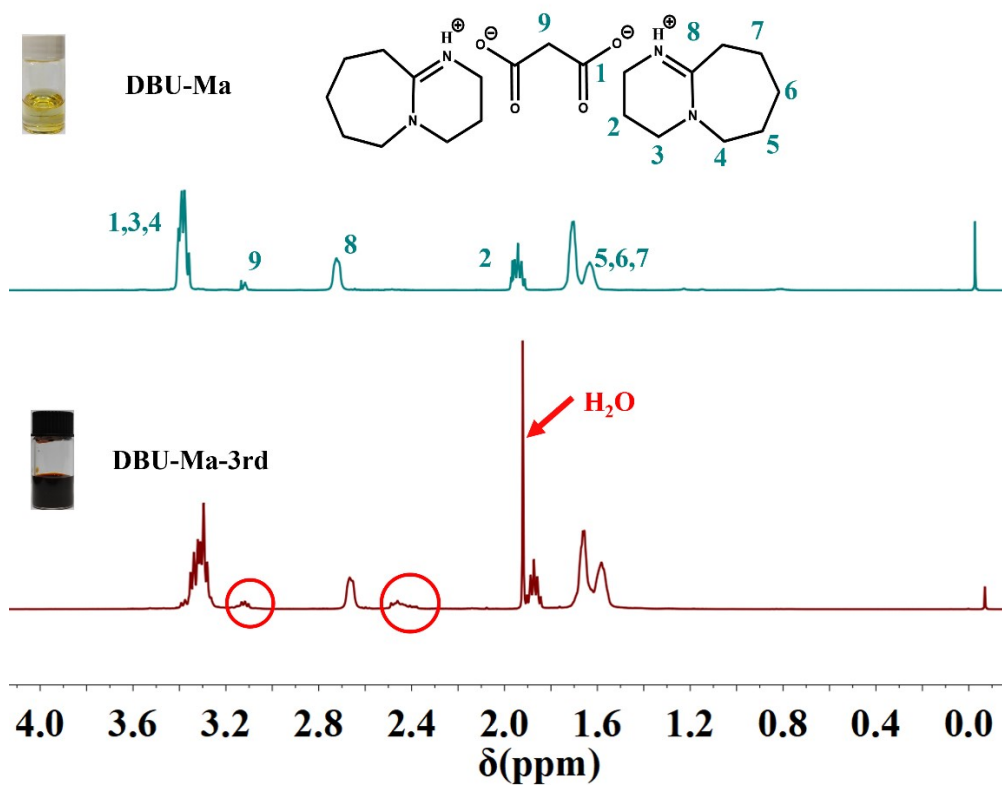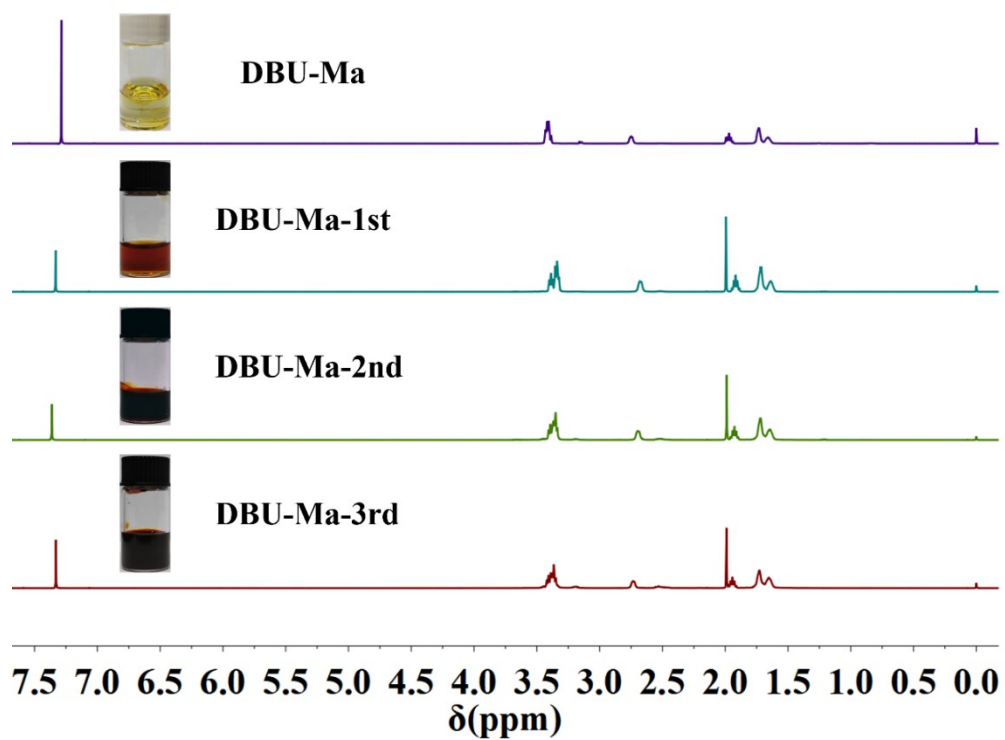
Figure S6. Photographs and ^{1}H NMR of DBU-Ma and recovered DBU-Ma.
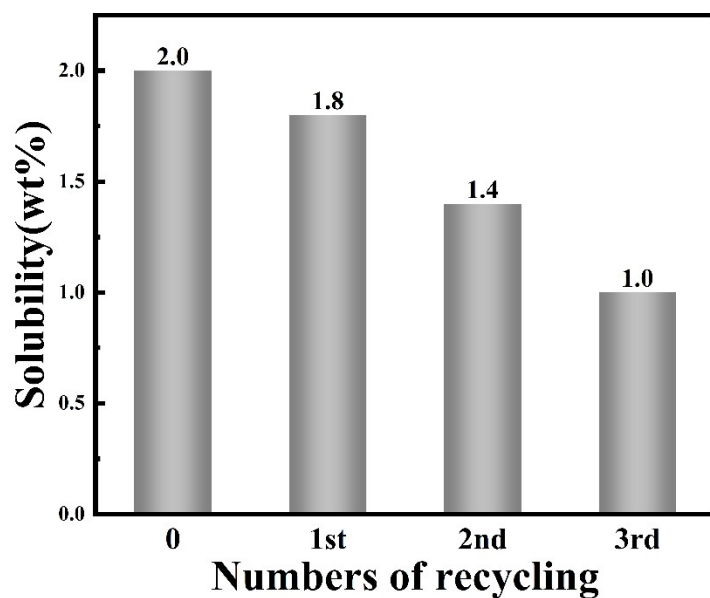
Figure S7. Solubility of recovered DBU-Ma for cellulose.
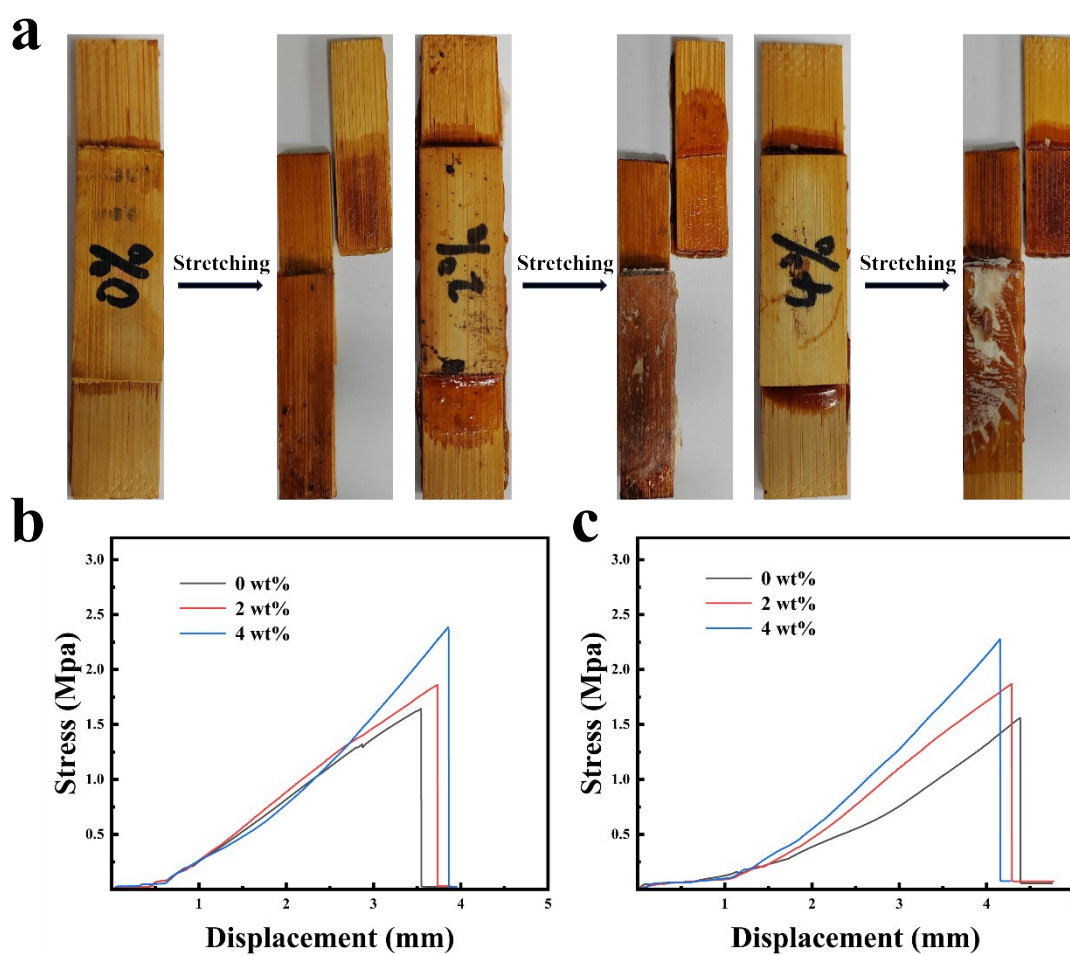
Figure S8. Photographs of adhesion of cellulose solution to bamboo panels (a), the stress-displacement curves of cellulose solutions to wood (b) and bamboo (c) panels.

S13
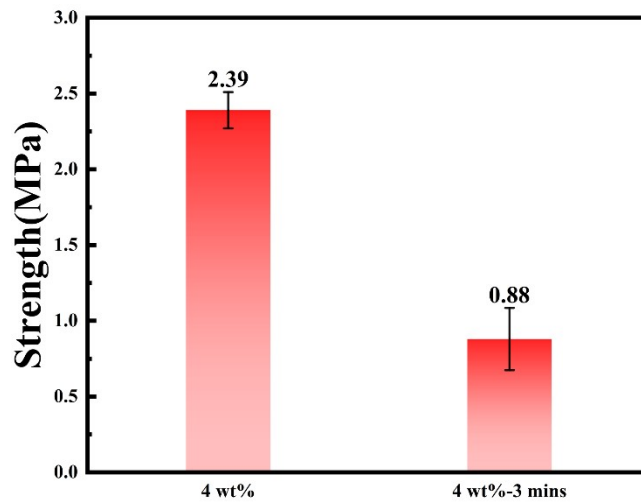
Figure S9. The tensile strengths of the wood panel soaked in water for 3 minutes and the wood panel without soaking in water.
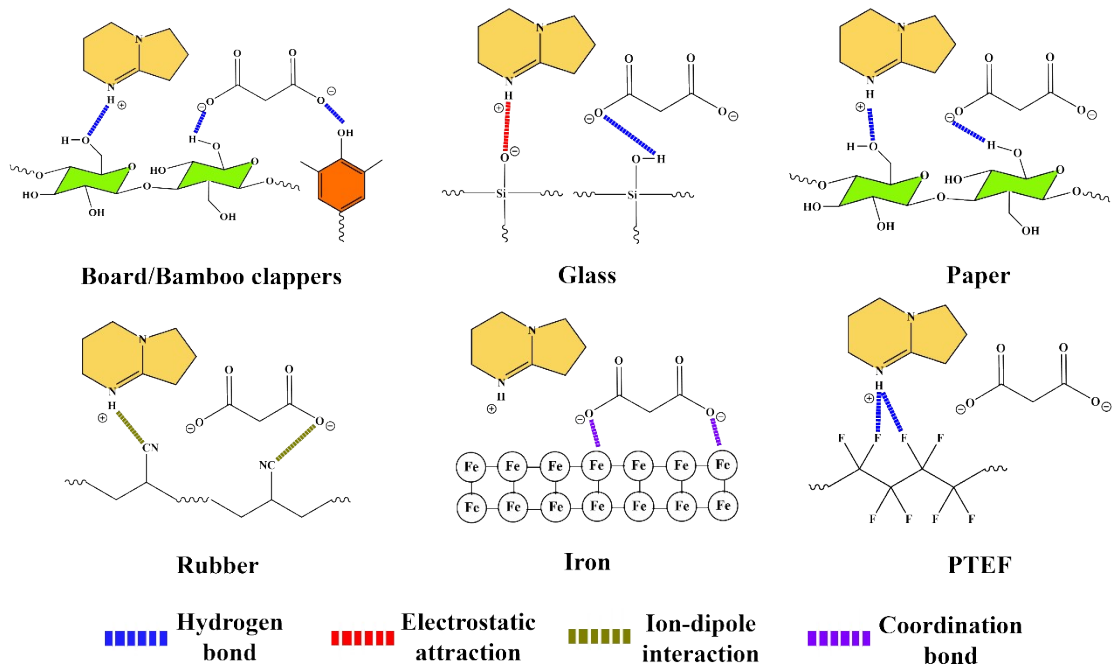
Figure S10. The adhesion mechanism of cellulose solutions to different substrates.
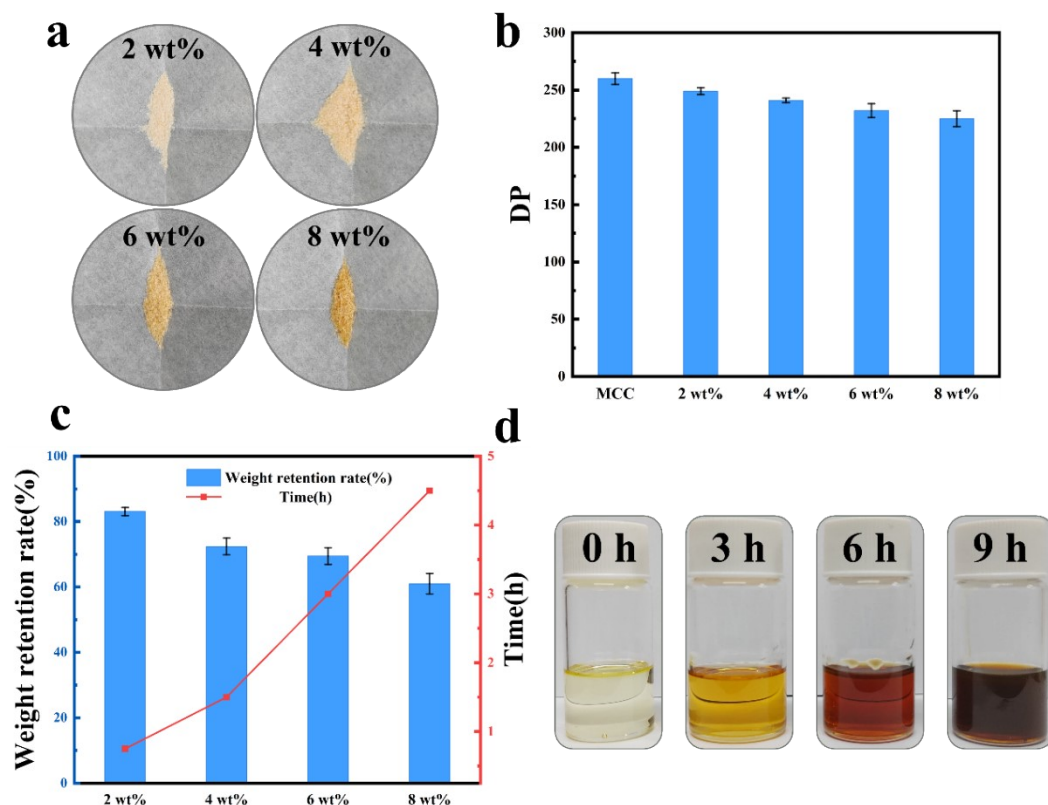
Figure S11. Photographs of regenerated cellulose with different concentrations (a), DP of regenerated cellulose with different concentrations (b), weight retention rate and heating time of regenerated cellulose with different concentrations (c), photographs of DBU-Ma with different heating times (d).
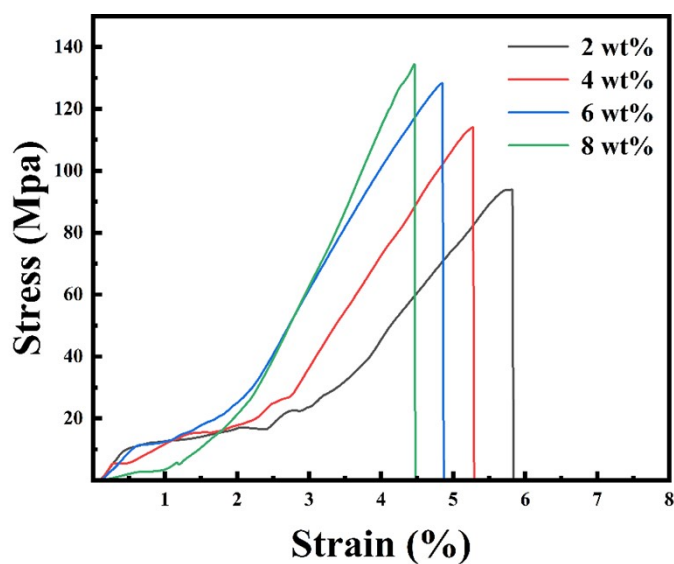
Figure S12. The stress-strain curves of cellulose films with different cellulose concentrations.
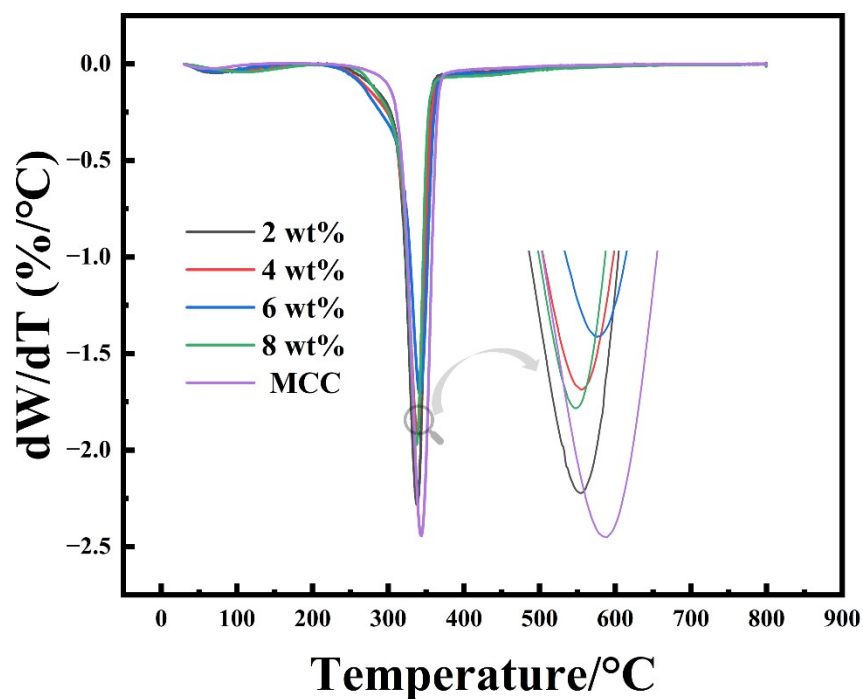
Figure S13. The DTG curves of cellulose films with different cellulose concentrations.

Figure S14. The physical photograph of ZHSC.
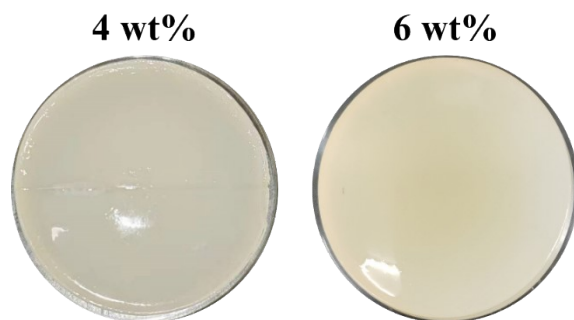
Figure S15. Photographs of 4 wt% and 6 wt% cellulose gels.
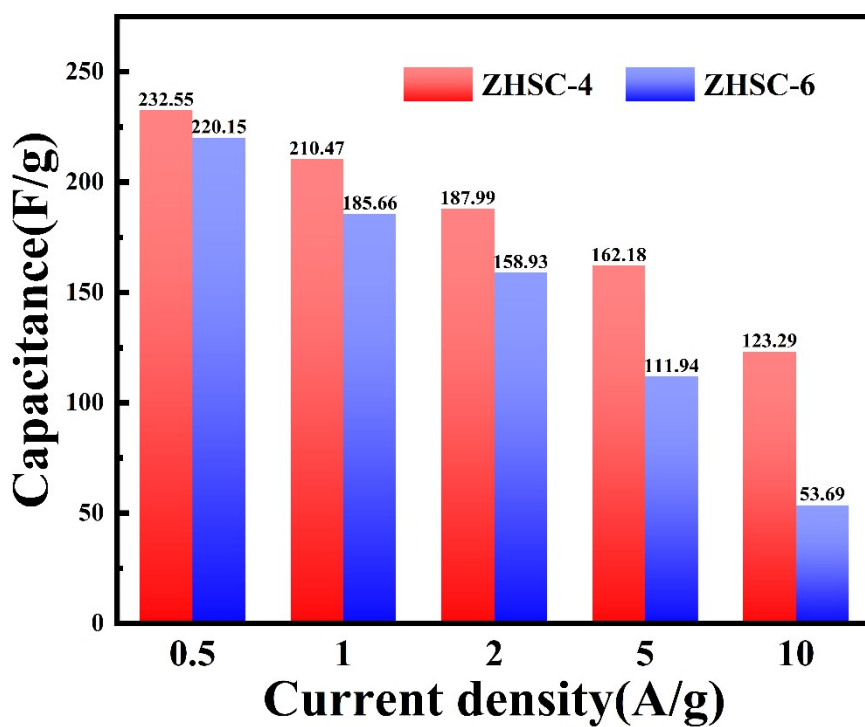
Figure S16. Capacitance of ZHSC-4 and ZHSC-6 at different current densities.
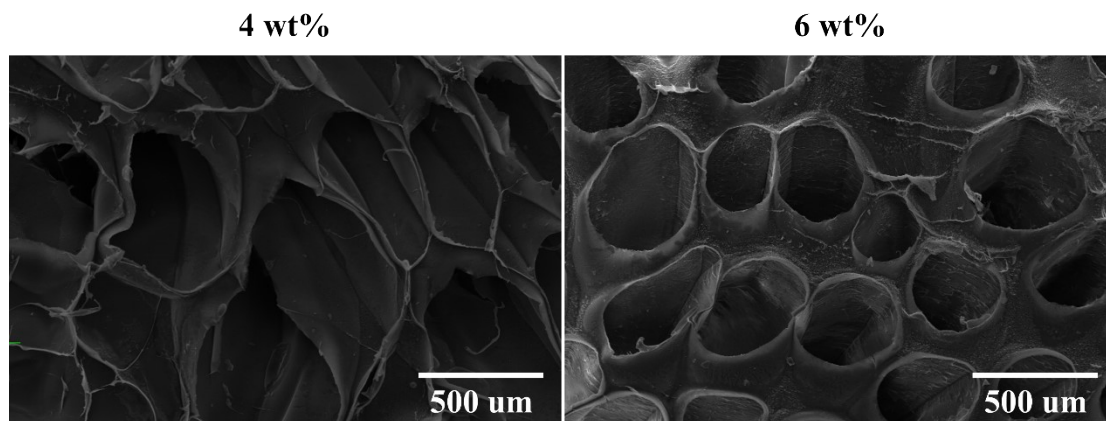
Figure S17. SEM photographs of 4 wt% and 6 wt% cellulose gels.

References

1. Y. H. Ci, T. Y. Chen, F. Y. Li, X. J. Zou and Y. J. Tang, *Int J Biol Macromol*, 2023, **252**, 126548.
2. Z. Liu, H. Wang, Z. X. Li, X. M. Lu, X. P. Zhang, S. J. Zhang and K. B. Zhou, *Mater Chem Phys*, 2011, **128**, 220-227.
3. S. C. He, J. T. Li, X. D. Cao, F. Xie, H. Yang, C. Wang, C. Bittencourt and W. J. Li, *Int J Biol Macromol*, 2023, **244**.
4. K. Chen, J. Huang, J. Yuan, S. Qin, P. Huang, C. Wan, Y. You, Y. Guo, Q. Xu and H. Xie, *Energy Storage Mater*, 2023, **63**, 102963.
5. M. Egal, T. Budtova and P. Navard, *Biomacromolecules*, 2007, **8**, 2282-2287.
6. J. P. Zhou and L. N. Zhang, *Polym J*, 2000, **32**, 866-870.
7. Q. H. Zhang, M. Benoit, K. D. Vigier, J. Barrault and F. Jérôme, *Chem-Eur J*, 2012, **18**, 1043-1046.
8. E. P. Zhou and H. R. Liu, *Asian J Chem*, 2014, **26**, 3626-3630.
9. H. W. Ren, C. M. Chen, S. H. Guo, D. S. Zhao and Q. H. Wang, *Bioresources*, 2016, **11**, 8457-8469.
10. H. W. Ren, C. M. Chen, Q. H. Wang, D. S. Zhao and S. H. Guo, *Bioresources*, 2016, **11**, 5435-5451.
11. J. G. Lynam, N. Kumar and M. J. Wong, *Bioresource Technol*, 2017, **238**, 684-689.
12. R. P. Swatloski, S. K. Spear, J. D. Holbrey and R. D. Rogers, *J Am Chem Soc*, 2002, **124**, 4974-4975.
13. H. Zhang, J. Wu, J. Zhang and J. S. He, *Macromolecules*, 2005, **38**, 8272-8277.
14. X. Zheng, F. Huang, L. H. Chen, L. L. Huang, S. L. Cao and X. J. Ma, *Carbohyd Polym*, 2019, **203**, 214-218.
15. A. R. Xu, L. Chen and J. J. Wang, *Macromolecules*, 2018, **51**, 4158-4166.
16. X. Li, H. C. Li, Z. Ling, D. X. Xu, T. T. You, Y. Y. Wu and F. Xu, *Macromolecules*, 2020, **53**, 3284-3295.